

Par3 and ZO-1 Membrane Clustering is an Indicator of Poor Prognosis in Lung Squamous Cell Carcinoma

Madoka NITO^{*1}, Susumu TAKEKOSHI^{*3}, Kanae KITATANI^{*2}, Tomohiko MATSUZAKI^{*1},
Hidehiko YAGASAKI^{*1}, Takaaki TSUBOI^{*1}, Kei NAKANO^{*1}, Kie SHIOYAMA^{*1},
Ryota MASUDA^{*1} and Masayuki IWAZAKI^{*1}

^{*1}*Division of Thoracic Surgery, Department of Surgery, Tokai University School of Medicine*

^{*2}*Support Center of Medical Reserch and Education, Tokai University School of Medicine*

^{*3}*Department of Cell Biology, Division of Host Defense Mechanism, Tokai University School of Medicine*

(Received January 6, 2021; Accepted April 1, 2021)

Epithelial cells form epithelial tissue structures by joining together *via* intercellular adhesion structures composed of intercellular adhesion factors such as zona occludins-1 (ZO-1). Epithelial cells are polarized at the apical and basal regions, and are bordered by intercellular adhesion structures called tight junctions; the organelles within epithelial cells are distributed asymmetrically. Maintenance of this asymmetry in normal epithelial cells is essential for normal cytoskeletal remodeling, movement, and cell division. The key factor regulating cell polarity is called partitioning-defective protein 3 (Par3). Abnormalities in cell polarity and intercellular adhesion are common features of many cancer tissues. Mutation and loss of cell polarity regulators contributes to the immortalization of normal cells and to the malignant transformation of cancer cells. In this study, we investigated the relationship between the subcellular localization of Par3 and ZO-1 and clinicopathological features of lung squamous cell carcinoma (lung SqCC). Both molecules were localized to the cell membrane in normal lung tissue, but the levels were lower at this location in pulmonary tumor tissue compared with normal lung tissue. Both Par3 and ZO-1 accumulated in clusters on the cell membrane (hereinafter, “foci”). Tumor size, recurrence rate, and mortality rate were significantly higher in patients with Par3 foci compared to those without Par3 foci. Rates of lymph node metastasis, recurrence, and mortality were significantly higher in patients with ZO-1 foci than in those without ZO-1 foci. The expression of *Par3* and *ZO-1* mRNA was not significantly different in samples from patients with foci versus those without. These results strongly suggest that the presence of Par3 and ZO-1 foci on the membrane may be a useful prognostic marker for lung SqCC.

Key words: cell polarity, Par3, ZO-1, lung cancer, squamous cell carcinoma (SqCC), foci

INTRODUCTION

Based on its histological characteristics, lung cancer is divided into small cell lung cancer (SCLC) and non-small cell lung cancer (NSCLC). The latter is further divided into adenocarcinoma (AC), squamous cell carcinoma (SqCC), and large cell carcinoma (LCC) subtypes. NSCLC is usually associated with a poor prognosis, and even in an early stage of the disease, many patients with NSCLC experience a recurrence despite surgical resection and radiation therapy [1]. The 5-year survival rate for lung cancer is only 60–70%, and there is an urgent need for more effective prophylactic measures, diagnostic procedures, and therapeutic approaches in order to treat this disease [2]. Chemotherapy for unresectable or recurrent lung cancer is more commonly used in AC than in SqCC [3]. In particular, the recent development of molecular-targeted therapies such as bevacizumab, erlotinib, and gefitinib have improved the outcome of AC treatment. In contrast, there is a lack of effective chemotherapies and molecular-targeted therapies for SqCC patients

with disease recurrence and in those whose disease outcome has a poor prognosis. In order to develop prognostic markers and therapeutic agents that contribute to improved treatment of SqCC, it is critical that we understand the underlying pathogenesis and associated biological features of the disease [4–6].

The cells that comprise multicellular organisms can be divided into epithelial and mesenchymal cells. Each epithelial cell adheres to neighboring cells *via* an adhesion complex that is supported by the cytoskeleton (i.e., actin and tubulin). There are different types of adhesion complexes, including tight junctions, adherens junctions, and desmosomes [7]. Being permanently bordered by tight junctions (TJ), epithelial cells are polarized by the presence of two regions with different functions, namely the apical and basolateral regions; this orientation helps to maintain tissue structure and function [8]. Defects in cell polarity are closely related to tumorigenesis [9]. Cell polarity-related molecules such as partitioning-defective proteins (Par), lethal giant larvae (Lgl, or Hvgl in humans), and atypical protein kinase C (aPKC) are involved in maintaining

the polarity of normal cells, and loss of function or abnormal expression of these molecules compromises cell polarity [10]. We previously reported that abnormalities in cell polarity-related molecules had an impact on survival and prognosis in patients with lung cancer. High levels of aPKC expression in lung AC were associated with significantly higher mortality, and apical membrane localization correlated with invasiveness and metastasis [11]. In patients with lung SqCC, low HUG1 expression was a prognostic factor for a high recurrence rate [12].

The *Par* genes were identified in a study analyzing asymmetric division mutants in fertilized eggs of *Caenorhabditis elegans*; six members, Par1 to Par6, have been reported so far. Par3 has three PDZ domains at the N-terminus that bind to various molecules, including activated Rac1 and Cdc42, which are small G proteins involved with the assembly of the actin cytoskeleton. Par3 also forms complexes (Par complexes) with Par6 and aPKC [13]. By binding to Rac1 and Cdc42 and regulating their activities, Par3 promotes the elongation of actin fibers and stabilizes them, thereby maintaining intercellular adhesion [14]. Par complexes are localized to TJ in the cell, where they regulate the process of intercellular adhesion. Knockdown of Par3 in cultured cells delocalizes ZO-1 from the cell membrane, reduces intercellular adhesion, and increases cell invasiveness [15]. Thus, Par3 likely suppresses abnormal motility by contributing to TJ stabilization [15]. Reduced Par3 expression is a feature of breast and pancreatic cancers [15, 16], suggesting that Par3 is important for tumorigenesis and malignant progression. Additionally, Par3 is mutated in the tissues of patients with lung SqCC, where it is accompanied by defective TJ formation of TJ. However, the relevance of Par3 aberrations to the prognosis of patients with SqCC remains to be clarified [17]. Par3 can regulate the Hippo/Yes-associated protein (YAP) signaling pathway in a manner that depends on the strength of TJ-mediated cell adhesion and cell density [18]. The Hippo/YAP signaling pathway is highly conserved in all organisms, and controls density-dependent cell division and organ size; the pathway includes the Lats1/2 proteins, which are tumor suppressors [19, 20]. This suggests that deregulated Hippo/YAP signaling due to the loss of Par3 function may be a tumor-initiating event.

In this study, we analyzed the relationship between abnormalities in the localization of Par3 and ZO-1 and the prognosis of SqCC. Our results highlight the importance of both molecules as novel prognostic markers in SqCC patients.

MATERIALS AND METHODS

Clinicopathological data

A total of 103 patients with lung SqCC who underwent resection at Tokai University Hospital (Kanagawa, Japan) between 2000 and 2010 were enrolled in this study. After informed consent was obtained from the patients, tissue samples were prepared from surgically excised specimens of lung SqCC and used for analysis. The histologic type was classified according to the World Health Organization (WHO) classification, and the tumor stage was classified according to the seventh edition of the TNM Classification of Malignant

Tumors published by the Union for International Cancer Control (UICC). The median postoperative follow-up period was 1,528 (41–3,837) days. This study was conducted with the approval of the institutional review board for clinical research, Tokai University Hospital. (IRB number: 11R-002).

Immunohistochemistry

Paraffin sections (4- μ m thick) were immersed in 0.01 M phosphate-buffered saline (PBS) after removal of the paraffin by xylene and ethanol. Endogenous peroxidase treatment was performed with 0.3% H₂O₂/MeOH solution. Antigen retrieval was carried out in 0.1 mM EDTA pH 8.0 solution in an autoclave at 121°C for 10 min. Anti-Par3 antibody (1:100; Millipore, Billerica, MA, USA) and anti-ZO-1 antibody (1:100; ThermoFisher Scientific, MA, USA) were each diluted in 1% BSA/PBS solution and incubated at 4°C overnight. After washing with PBS five times, the Simple Stain anti-rabbit antibody (Nichirei Biosciences, Japan) was reacted for 1 h at room temperature. After washing with PBS five times, chromogenic reaction was performed using 3'3'-diaminobenzidine tetrahydrochloride (DAB). For double staining of Par3 and ZO-1, antigen retrieval and endogenous peroxidase treatment were carried out in the same manner as above, and incubated with anti-Par3 antibody overnight at 4°C. Subsequently, the secondary antibody was incubated as described above and (after chromogenic reaction with DAB), the residual primary antibody was removed using glycine-hydrochloric acid buffer solution. For secondary staining, the anti-ZO-1 antibody was incubated at 4°C in the same manner as single staining, and then samples were incubated with the Simple Stain anti-rabbit antibody. A chromogenic reaction was performed using Fast Blue RR Salt (Sigma-Aldrich, St. Louis, MO, USA) and naphthol AS-BI phosphate disodium salt (Sigma-Aldrich).

Quantitative real-time RT-PCR

Normal or tumor specimens were excised from paraffin tissue sections (4- μ m thick) using a scalpel. Total RNA was extracted using the RNeasy FFPE kit (QIAGEN, Hilden, Germany), followed by cDNA synthesis using the High Capacity cDNA Reverse Transcription Kit (Applied Biosystems, CA, USA). Real-time PCR was performed using TaqMan Universal PCR Master Mix (Applied Biosystems) and TaqMan Gene Expression Assays (Par3: Hs00969077_m1; GAPDG: Hs02786624_g1; Applied Biosystems). PCR was performed using the Opticon 2 System (BioRad, CA, USA) at 95°C for 15 min, 95°C for 15 s, and 60°C for 1 min for 40 cycles. All data were analyzed using the Opticon Monitor 3 software (BioRad, CA, USA). Par3 expression levels were calculated using the CT method.

Statistical analysis

A p value of less than 0.05 was considered to indicate a statistically significant difference in univariate analyses (Chi-square test and Student's *t*-test). Survival time was defined as the time from the day of surgery to the day of death from any cause. The relationship with survival rate was evaluated using Kaplan-Meier survival curves. All analyses were performed using

Table 1 Clinicopathological characteristics of the SqCC cases

| | | |
|--------------------------------|-----------------------------|------------|
| Age(years) | | 68 (43–85) |
| Gender | Male/Female | 97/6 |
| Smoking | smoking/non-smoking/unknown | 36/18/49 |
| Pre-operative chemotherapy | positive/negative/unknown | 0/103/0 |
| Pre-operative radiationtherapy | positive/negative/unknown | 1/102/0 |
| Par3 | positive/negative/unknown | 91/12/0 |
| ZO-1 | positive/negative/unknown | 82/21/0 |

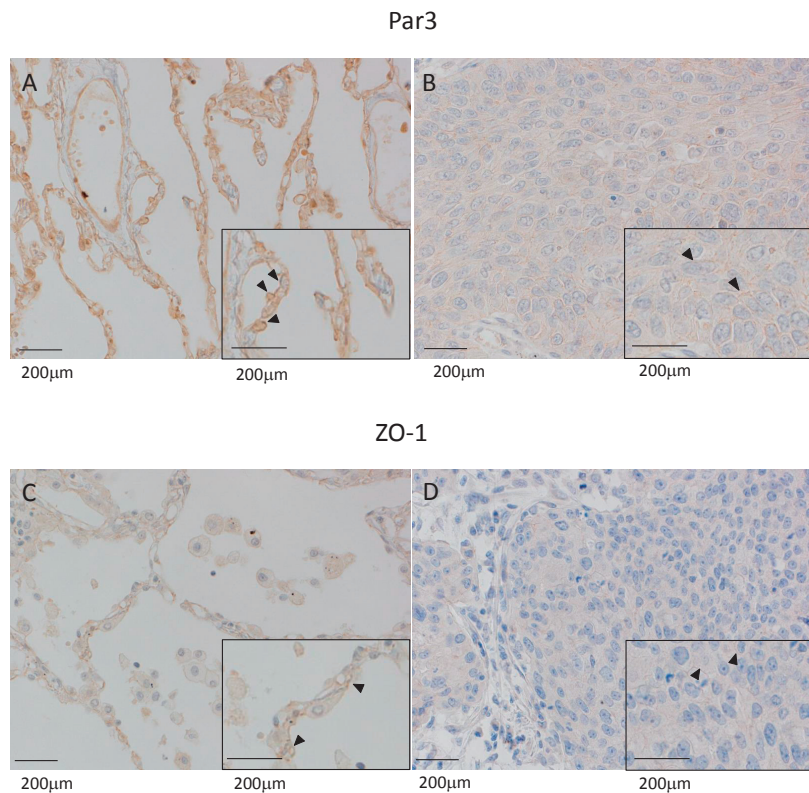


Fig. 1 Immunohistochemical images of normal and tumor sites in human lung tissue (magnification: $\times 100$)
 (A) Par3 staining in normal tissue. The lower right photo is an enlarged view, and the arrowhead shows Par3.
 (B) Par3 staining in tumor tissue. The lower right photo is an enlarged view, and the arrowhead shows Par3.
 (C) ZO-1 staining in normal tissue. The lower right photo is an enlarged view, and the arrowhead shows ZO-1.
 (D) ZO-1 staining in tumor tissue. The lower right photo is an enlarged view, and the arrowhead shows ZO-1.

IBM SPSS Statistics (version 24; IBM Japan, Japan).

RESULTS

Clinicopathological features of patients

Clinical and histopathological variables are shown in Table 1. The group consisted of 97 men and six women aged 43 to 85 years (median age: 68 years). The maximum tumor diameter ranged from 6 to 95 mm, with a median diameter of 35 mm. Of the 103 patients, two had stage 0 disease, 25 had stage IA, 28 had stage IB, 18 had stage IIA, 10 had stage IIB, 17 had stage IIIA, one had stage IIIB, and two had stage IV (UICC pathological TNM [pTNM] classification, version 7).

Correlation between subcellular localization of Par3 and ZO-1 and clinicopathological features

Immunohistochemistry revealed differences in the localization of Par3 and ZO-1, a TJ marker, at the tumor site. The cell membrane of normal squamous epithelial tissue was strongly positive for Par3 (Fig. 1A), but staining was weaker in tumor tissue, where it was observed in both the cellular membrane and the cytoplasm (Fig. 1B). ZO-1 was uniformly localized to the cell membrane in normal tissue (Fig. 1C), but this consistency was absent at the tumor site (Fig. 1D). Within the group, there was some variation in the subcellular and membrane localization of Par3. In some cases, localization to the cell membrane was observed, yet partial accumulation and resultant focal formation were present (Fig. 2A, Par3 foci +), while in other

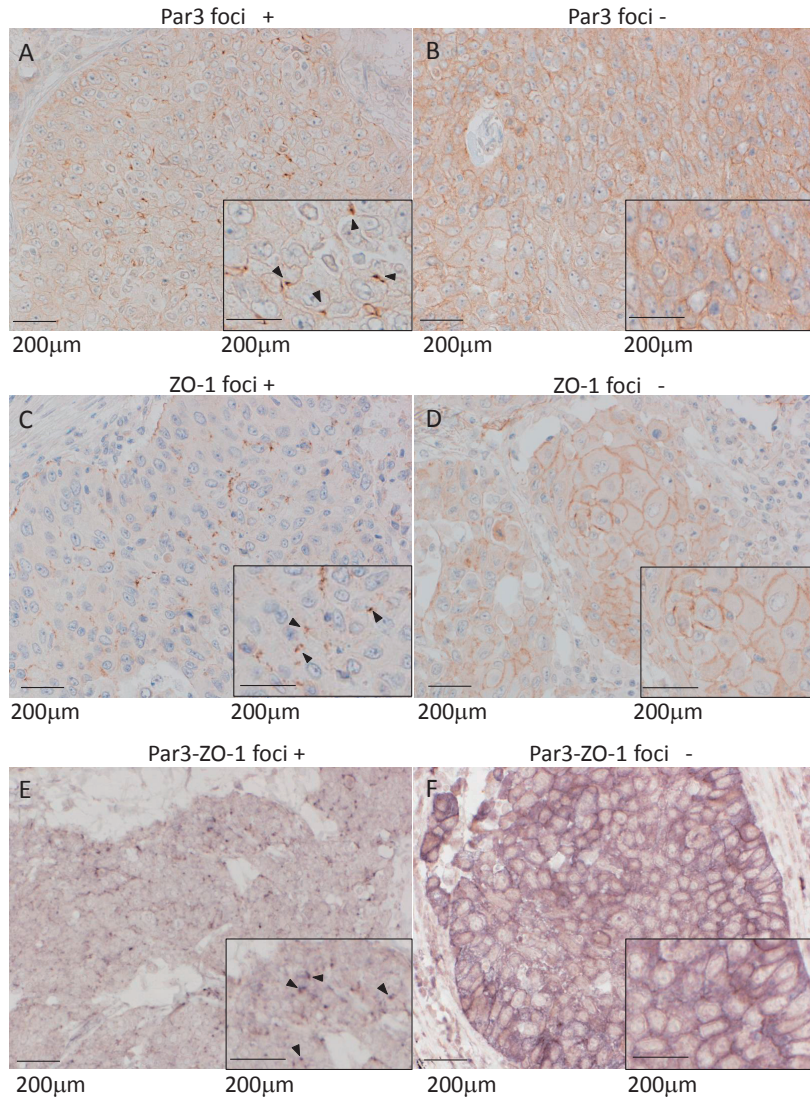


Fig. 2 Abnormal accumulation of Par3 and ZO-1 by immunohistochemistry at the tumor site in human lung tissue (magnification: $\times 100$)

- (A) Case with abnormal accumulation of Par3 (foci group) The lower right photo is an enlarged view, and the arrowhead shows Par3 foci.
- (B) Case without abnormal accumulation of Par3 (no-foci group) The lower right photo is an enlarged view.
- (C) Case with abnormal accumulation of ZO-1 (foci group) The lower right photo is an enlarged view, and the arrowhead shows ZO-1 foci.
- (D) Case without abnormal accumulation of ZO-1 (no-foci group) The lower right photo is an enlarged view.
- (E) Case with abnormal accumulation on double staining of Par3 (brown) and ZO-1 (blue) (foci group) Arrowheads indicate Par3 and ZO-1 foci.
- (F) Case without abnormal accumulation on double staining of Par3 (brown) and ZO-1 (blue) (no-foci group) The lower right photo is an enlarged view.

cases, uniform localization was noted (Fig. 2B, Par3 foci -). As with Par3, ZO-1 localization was different in tumor compared to normal tissue. Specifically, in some cases, localization to the cell membrane was observed, yet partial accumulation and resultant focal formation were also present (Fig. 2C, ZO-1 foci +), while in other cases, uniform localization was noted (Fig. 2D, ZO-1 foci -). Double staining revealed abnormal localization of ZO-1 at the membrane in Par3 foci-positive cases (Fig. 2E and F).

Based on the results of immunohistochemical staining, the samples were divided into two groups: one with uniform staining in the cytoplasm or membrane (no-foci group); and the other with localization to the membrane along with partial accumulation and resultant focal formation (foci group). These were then

subjected to statistical analysis. Univariate analysis by chi-square test revealed a significantly larger tumor diameter ($p = 0.027$), significantly higher recurrence rate ($p = 0.010$), and significantly higher mortality rate ($p = 0.017$) in the Par3 foci group than in the no Par3 foci group (Table 2). There was no association with other clinicopathological parameters (Table 2). In addition, Kaplan-Meier analysis showed that survival time was significantly shorter in the foci group than in the no-foci group (Fig. 3A). As for ZO-1, the rates of lymph node metastasis, recurrence, and mortality were significantly higher in the foci group than in the no-foci group ($p = 0.005$, 0.038 , and 0.027 , respectively) (Table 3). Survival time was also significantly shorter in the foci group ($p = 0.018$) (Fig. 3B).

Table 2 Clustering (foci) of Par3 and clinicopathological features

| variable | n (%) | Par3 foci | | X ² |
|------------------------------|-----------|-----------|----------|----------------|
| | | negative | positive | |
| Age of surgery | | | | |
| < 68 | 36(39.6) | 23 | 13 | |
| ≥68 | 55(60.4) | 24 | 31 | 0.059 |
| Gender | | | | |
| Male | 85(93.4) | 32 | 53 | |
| Female | 6(6.6) | 4 | 2 | 0.160 |
| Tumor size | | | | |
| < 30mm | 33(36.3) | 18 | 15 | |
| ≥30cm | 58(63.7) | 18 | 40 | 0.027 |
| Lymph node metastasis | | | | |
| negative | 40(44.4) | 20 | 20 | |
| Positive | 50(55.6) | 15 | 35 | 0.053 |
| Venous invasion | | | | |
| negative | 46(51.7) | 22 | 24 | |
| Positive | 43(48.3) | 13 | 30 | 0.090 |
| Histological differentiation | | | | |
| Well, Moderate | 79(86.8) | 32 | 47 | |
| Poor | 12(13.2) | 4 | 8 | 0.636 |
| Stage | | | | |
| I, II | 73(80.2) | 33 | 40 | |
| III, IV | 18(19.8) | 4 | 14 | 0.075 |
| Recurrence | | | | |
| R0 | 44(60.3) | 24 | 20 | |
| R1, R2 | 29(39.7) | 7 | 22 | 0.010 |
| Survival | | | | |
| Alive | 41(56.2) | 23 | 18 | |
| Dead | 32 (43.8) | 9 | 23 | 0.017 |

Table 3 Clustering (foci) of ZO-1 and clinicopathological features

| variable | n (%) | ZO-1 foci | | X ² |
|------------------------------|----------|-----------|----------|----------------|
| | | negative | positive | |
| Age of surgery | | | | |
| < 68 | 44(53.7) | 24 | 20 | |
| ≥68 | 38(46.3) | 17 | 21 | 0.376 |
| Gender | | | | |
| Male | 76(92.7) | 37 | 39 | |
| Female | 6(7.3) | 4 | 2 | 0.396 |
| Tumor size | | | | |
| < 30mm | 31(37.8) | 18 | 13 | |
| ≥30cm | 51(62.2) | 23 | 28 | 0.255 |
| Lymph node metastasis | | | | |
| negative | 38(46.9) | 25 | 13 | |
| Positive | 43(53.1) | 15 | 28 | 0.005 |
| Venous invasion | | | | |
| negative | 44(55.0) | 25 | 19 | |
| Positive | 36(45.0) | 15 | 21 | 0.178 |
| Histological differentiation | | | | |
| Well, Moderate | 71(86.6) | 36 | 35 | |
| Poor | 11(13.4) | 5 | 6 | 0.746 |
| Stage | | | | |
| I, II | 65(79.3) | 33 | 32 | |
| III, IV | 17(20.7) | 8 | 9 | 0.785 |
| Recurrence | | | | |
| R0 | 53(64.6) | 31 | 22 | |
| R1, R2 | 29(35.4) | 10 | 19 | 0.038 |
| Survival | | | | |
| Alive | 40(48.8) | 25 | 15 | |
| Dead | 42(51.2) | 16 | 26 | 0.027 |

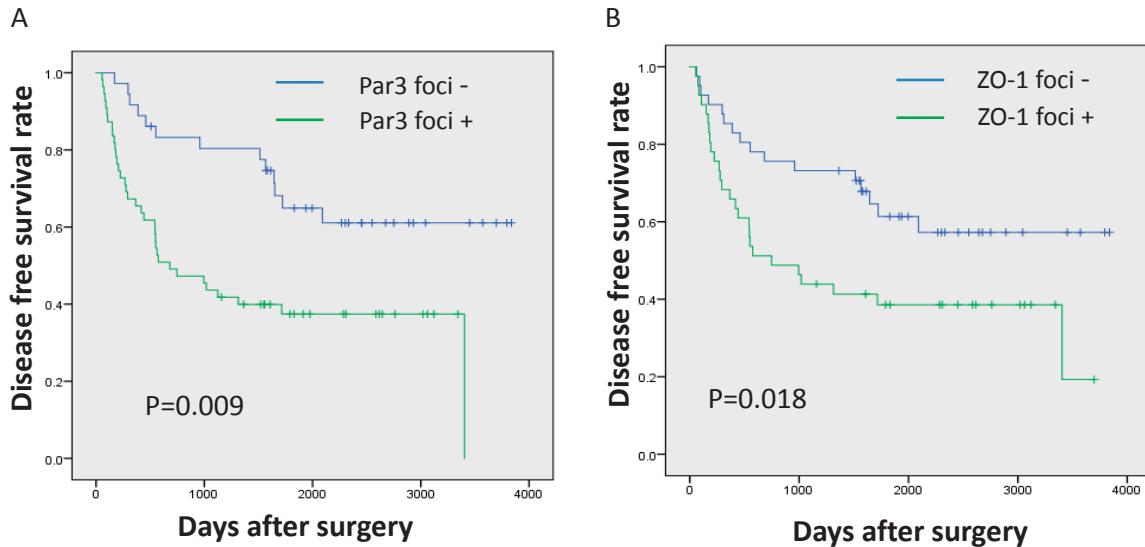


Fig. 3 Kaplan-Meier survival curves for Par3 and ZO-1
 (A) Comparison of the group with abnormal accumulation of Par3 (foci group) and the no-foci group
 (B) Comparison of the group with abnormal accumulation of ZO-1 (foci group) and the no-foci group

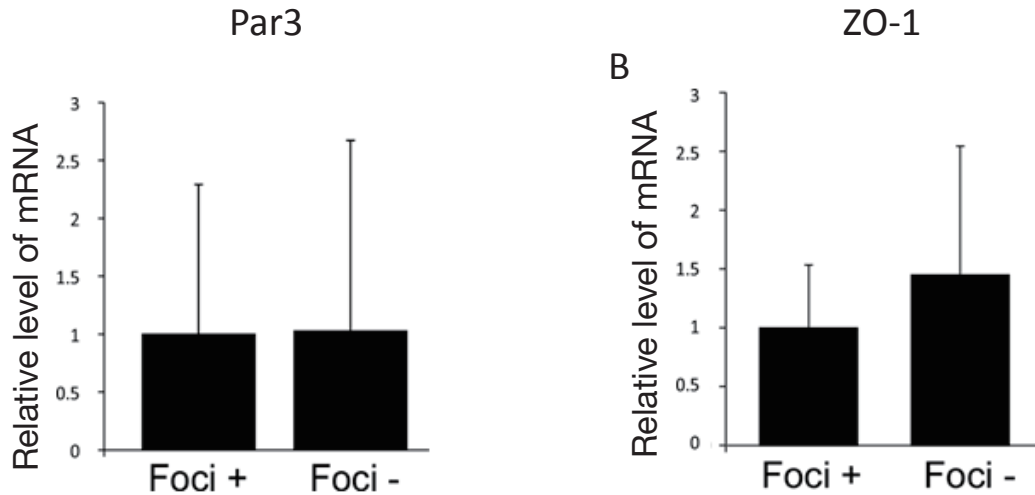


Fig. 4 Real-time RT-PCR analysis of Par3 and ZO-1 expression levels in human lung tumor tissue
 (A) Comparison of the expression levels of Par3 between the foci group and the no-foci group
 (B) Comparison of the expression levels of ZO-1 between the foci group and the no-foci group

Analysis of Par3 and ZO-1 mRNA expression

Quantitative real-time PCR was used to examine whether differences in the localization of Par3 and ZO-1 correlated with their expression levels. No clear difference in *Par3* expression was found between the foci group and the no-foci group (Fig. 4A). Similarly, *ZO-1* expression did not differ between the foci and no-foci groups (Fig. 4B). Thus, there was no correlation between the formation of foci and the expression of *Par3* and *ZO-1* mRNA.

DISCUSSION

Our results demonstrated that abnormalities in the subcellular localization of Par3 were strongly associated with postoperative recurrence and mortality in patients with SqCC. While the overall 5-year survival rate was 47.3% (n = 103 patients), it was significantly lower (only 36.4%) for patients with Par3 foci (p = 0.003)(Table 1). The level of *Par3* mRNA expression was not associated with differences in subcellular localization (Fig. 4A,

B), suggesting that mRNA quantification has limited prognostic utility. Among the total of 103 patients, 34 had recurrent disease, and samples from 29 of these patients were positive for Par3 foci. The recurrence rate was significantly higher in these 29 patients than in those without foci (p = 0.010). Membrane clustering of ZO-1, a TJ marker, was associated with significantly higher rates of lymph node metastasis (p = 0.005), recurrence (p = 0.038), and mortality (p = 0.027) when compared to the no-foci group (Table 2). Double staining of Par3 and ZO-1 revealed that ZO-1 was partially localized to the membrane in Par3 foci-positive cases; in these samples, TJ formation was defective (Fig. 2E). These results suggest that Par3 and ZO-1 foci are reliable markers for estimating prognosis after surgery for SqCC. So far, there have been no reports showing the relationship between the localization of Par3 and ZO-1 with the prognosis of SqCC. In what we believe is the first such report, we show here that the membrane clustering of Par3 and ZO-1 is associated with poor

prognosis in SqCC.

Disruption of polarity in epithelial cells can lead to neoplasia in many organs [9]. Consistent with a report of an association between abnormalities in cell polarity factors and carcinogenesis in the lung [21], we previously reported that the expression of HUG1, a cell polarity molecule, was inversely correlated with the survival rate of patients with lung SqCC [12]. In the present study, we clarified the relationship between the cell membrane localization of Par3 and the survival rate of lung SqCC patients. Par3 is a tumor suppressor, and it has been reported that genetic loss of function are associated with transformation of normal cells and/or an increase in tumor malignancy [17]. Par3 can also suppress cell motility and abnormal proliferation, and plays a role in maintaining normal tissue. Examples include the development of keratoacanthoma in Par3 knockout mice [22] and enhancement of the growth and metastatic potential of breast and pancreatic cancers as a result of Par3 deficiency [16, 17]. A study using lung SqCC tissues found expression of multiple Par3 splice variants that induced in-frame deletions or missense amino acid Par3 variants. Unlike wild type Par3, these variants (PDZ domain deletion, aPKC binding domain mutation, and FRMD4a [scaffold protein] binding domain mutation) were unable to inhibit cell proliferation [18]. Our study showed no association between the expression level of Par3 and clinicopathological features. This suggests that the expression of the splicing variants of Par3 or mutant Par3 in lung SqCC may have engendered cell polarity abnormalities, leading to increased malignancy and poor prognosis. Furthermore, expression of the splicing variant of Par3 is associated with abnormalities in cell polarity and proliferation [23]. The Hippo/YAP signaling pathway regulates tissue size by inducing cell division and apoptosis in a cell density-dependent manner [20]. It has been reported that Par3 lacking the third PDZ domain cannot bind to YAP. This leads to YAP hyperphosphorylation, which in turn enhances intranuclear translocation and YAP-driven transcription of cell growth-related factors [19]. Par3 promotes the localization of intercellular adhesion proteins such as E-cadherin and polar proteins to the apical region during early embryogenesis in *C. elegans*. However, approximately 20% of *C. elegans* larvae that express a splice variant of Par3 lacking the first PDZ domain (tm2716) die at the L1 stage, and the expression of Par3 lacking the PDZ domain may trigger loss of normal cell polarity [24].

The analysis of Par3 and ZO-1 mRNA expression revealed no difference in their expression levels between the foci group and the no-foci group. Both molecules play important roles in cell-cell adhesion. However, in the foci group, Par-3 and ZO-1 were aberrantly localized, suggesting dysfunction of both molecules. Stabilization of intercellular adhesion inhibits cell motility and proliferation, whereas cancerous cells exhibit abnormal intercellular adhesion. Membrane localization of intercellular adhesion factors such as ZO-1 is lost in MDCK-II cells following Par3 knockdown, demonstrating that Par3 is necessary for TJ maturation [13]. Expression of a non-functional mutant form of Par3 in lung SqCC presumably prevents TJ maturation, leading to enhanced metastatic poten-

tial. Defective intercellular adhesion also causes epithelial-mesenchymal transition [25] and is associated with carcinogenesis. In this study, aggregates of ZO-1 were localized to the membrane in the same way as Par3, and this was associated with mortality. Dysfunction of Par3 leads to defective TJ formation and abnormal cell polarity, thus promoting the malignant transformation of lung SqCC. We previously reported that excessive activation of aPKC induced by oxidative stress resulted in Par3 phosphorylation and defective TJ formation [26]. Furthermore, Par3 knockdown increases the motility and outgrowth potential of lung AC cells [27]. In this study, we could not fully examine the expression of Par3 mutations and splicing variants due to a lack of patient material. Further research is warranted to clarify the relationship between the presence or absence of Par3 and its expression of splicing variants and the clinicopathological features of patients with lung SqCC.

Tyrosine kinase inhibitors for EGFR, ROS1, ALK, PDL-1, BRAF have been developed as molecular-targeted therapeutic agents for AC. In contrast, there are no clear driver-linked mutations in SqCC, and therefore there is a lack of molecular-targeted therapeutic agents to treat this malignancy [28]. In our current study, we found that the abnormal localization (clustering) of Par3 and ZO-1 is related to the prognosis in SqCC. Par3 and ZO-1 foci may be useful prognostic markers for lung SqCC. We speculate that the abnormal localization of both molecules in SqCC leads to their dysfunction, which in turn affects cell motility and proliferation. Therefore, we suggest that the development of drugs that complement or enhance the functions of Par3 and/or ZO-1 will be advantageous for treatment of SqCC.

ACKNOWLEDGMENTS

The authors wish to thank Ms. Yoshiko Itoh and Ms. Youko Kameyama (Support Center for Medical Research and Education, Tokai University) for technical assistance with immunohistochemical analysis.

REFERENCES

- 1) Ferlay J, Shin HR, Bray F, Forman D, Mathers C, Parkin DM. Estimates of worldwide burden of cancer in 2008: GLOBOCAN 2008. *International journal of cancer* Journal international du cancer 2010; 127: 2893-2917.
- 2) Goldstraw P, Crowley J, Chansky K, Giroux DJ, Groome PA, Rami-Porta R *et al.* The IASLC Lung Cancer Staging Project: proposals for the revision of the TNM stage groupings in the forthcoming (seventh) edition of the TNM Classification of malignant tumours. *Journal of thoracic oncology: official publication of the International Association for the Study of Lung Cancer* 2007; 2: 706-714.
- 3) Huang Y, Zhang L, Shi Y, Ma S, Liao M, Bai C, *et al.* Efficacy of erlotinib in previously treated patients with advanced non-small cell lung cancer: analysis of the Chinese subpopulation in the TRUST study *Jpn J Clin Oncol* 2015; 45: 6, 569-575.
- 4) Hong J, Kyung SY, Lee SP, Park JW, Jung SH, Lee JI *et al.* Pemetrexed versus gefitinib versus erlotinib in previously treated patients with non-small cell lung cancer. *The Korean journal of internal medicine* 2010; 25: 294-300.
- 5) Sandler A, Gray R, Perry MC, Brahmer J, Schiller JH, Dowlati A *et al.* Paclitaxel-carboplatin alone or with bevacizumab for non-small-cell lung cancer. *The New England journal of medicine* 2006; 355: 2542-2550.
- 6) Rosell R, Perez-Roca L, Sanchez JJ, Cobo M, Moran T, Chaib I *et al.* Customized treatment in non-small-cell lung cancer based

- on EGFR mutations and BRCA1 mRNA expression. *PLoS one* 2009; 4: e5133.
- 7) Balda MS, Matter K. Tight junctions as regulators of tissue remodelling. *Current Opinion in Cell Biology*. 2016 42: 94-101.
 - 8) Shin K, Fogg VC, Margolis B. Tight Junctions and Cell Polarity. *Annu. Rev. Cell Dev. Biol.* 2006. 22: 207-235.
 - 9) Halaoui R, McCaffrey L. Rewiring cell polarity signaling in cancer. *Oncogene*. 2015. 34, 939-950.
 - 10) Spaderna S, Schmalhofer O, Wahlbuhl M, Dimmler A, Bauer K, Sultan A *et al.* The transcriptional repressor ZEB1 promotes metastasis and loss of cell polarity in cancer. *Cancer research* 2008; 68: 537-544.
 - 11) Imamura N, Horikoshi Y, Matsuzaki T, Toriumi K, Kitatani K, Ogura G *et al.* Localization of aPKC Lambda/Iota and Its Interacting Protein, Lgl2, Is Significantly Associated with Lung Adenocarcinoma Progression. *Tokai J Exp Clin Med.* 2013;Vol. 38, No. 4: 146-158.
 - 12) Matsuzaki T, Takekoshi S, Toriumi K, Kitatani K, Nitou M, Imamura N *et al.* Reduced Expression of HUGL 1 Contributes to the Progression of Lung Squamous Cell Carcinoma. *Tokai J Exp Clin Med.* 2015; Vol. 40, No. 4: 169-177.
 - 13) Ooshio T, Fujita N, Yamada A, Sato T, Kitagawa Y, Okamoto R, *et al.* Cooperative roles of Par-3 and afadin in the formation of adherens and tight junctions. *J Cell Sci.* 2007; 120(Pt 14): 2352-2365.
 - 14) Goldstein B, Macara IG. The PAR Proteins: Fundamental Players in Animal Cell Polarization. *Dev Cell.* 2007; 13(5): 609-22.
 - 15) Itoh M, Sasaki H, Fruse M, Ozaki H, Kita T, Tsukita S. Junctional adhesion molecule (JAM) binds to PAR-3: a possible mechanism for the recruitment of PAR-3 to tight junctions. *J Cell Biol.* 2001; 154(3): 491-497.
 - 16) Guo X, Wang M, Zhao Y, Wang X, Shen M, Zhu F *et al.* Par3 regulates invasion of pancreatic cancer cells via interaction with Tiam1. *Clin Exp Med.* 2016; 16: 357-365.
 - 17) Archibald A, Mihai C, Macara IG, McCaffrey L. Oncogenic suppression of apoptosis uncovers a Rac1/JNK proliferation pathway activated by loss of Par3. *Oncogene.* 2015; 34: 3199-3206.
 - 18) Bonastre E, Verdura S, Zondervan I, Facchinetti F, Lantuejoul S, Chiara MD *et al.* PARD3 Inactivation in Lung Squamous Cell Carcinomas Impairs STAT3 and Promotes Malignant Invasion. *Cancer Res* 2015; 75: 1287-1297.
 - 19) Zhang P, Wang S, Wang S, Qiao J, Zhang L, Zhang Z *et al.* Dual function of partitioning-defective 3 in the regulation of YAP phosphorylation and activation. *Cell Discovery* 2016; 2, 16021: 1-17.
 - 20) Ferraiuolo M, Verduci L, Blandino G, Strano S. Mutant p53 Protein and the Hippo Transducers YAP and TAZ: A Critical Oncogenic Node in Human Cancers. *Int. J. Mol. Sci.* 2017; 18, 961.
 - 21) Bonastre E, Brambilla E, Sanchez-Cespedes M. Cell adhesion and polarity in squamous cell carcinoma of the lung. *J Pathol* 2016; 238: 606-616.
 - 22) Iden S, Van Riel WE, Schafer R, Song JY, Hirose T, Ohno S *et al.* Tumor Type-Dependent Function of the Par3 Polarity Protein in Skin Tumorigenesis. *Cancer Cell.* 2012. 22, 389-403.
 - 23) Yoshii T, Mizuno K, Hirose T, Nakajima A, Sekihara H, Ohno S. sPAR-3, a splicing variant of PAR-3, shows cellular localization and an expression pattern different from that of PAR-3 during enterocyte polarization. *Am. J. Physiol Gastrointest Liver Physiol.* 2005; 288: G564-G570.
 - 24) Achilleos A, Wehman AM, Nnce J. PAR-3 mediates the initial clustering and apical localization of junction and polarity proteins during *C. elegans* intestinal epithelial cell polarization. *Development.* 2010; 137, 1833-1842.
 - 25) Björn B LDM, Jamall IS. Cell-Cell Communication in the Tumor Microenvironment, Carcinogenesis, and Anticancer Treatment. *Cell Physiol Biochem* 2014; 34: 213-243.
 - 26) Horikoshi Y, Kitatani K, Toriumi K, Fukunishi N, Itoh Y, Nakamura N *et al.* Aberrant Activation of Atypical Protein Kinase C in Carbon Tetrachloride-induced Oxidative Stress Provokes a Disturbance of Cell Polarity and Sealing of Bile Canalicular Lumen. *The American Journal of Pathology*, 2015; Vol. 185, No. 4.
 - 27) Song T, Tian X, Kai F, Ke J, Wei Z, Jing-Song L *et al.* Loss of Par3 promotes lung adenocarcinoma metastasis through 14-3-3 ζ protein. *Oncotarget.* 2016; 27; 7(39): 64260-64273.
 - 28) The Cancer Genome Atlas Research Network. Comprehensive genomic characterization of squamous cell lung cancers. *Nature*, 2012; 489(7417): 519-25.